UCRL - 76438
PREPRINT
Conf-750607--13

LAWRENCE LIVERMORE LABORATORY
University of California/Livermore, California

FUSION PLASMA LOSSES DUE TO THE CHARGE EXCHANGE OF INJECTED NEUTRALS

David J. Bender and Gustav A. Carlson

April 1, 1975

This Paper Was Prepared for Presentation at the
American Nuclear Society Annual Meeting
New Orleans, June 8-13, 1975

FUSION PLASMA LOSSES DUE TO THE CHARGE EXCHANGE OF INJECTED NEUTRALS*

David J. Bender and Gustav A. Carlson

Lawrence Livermore Laboratory

ABSTRACT

The interaction of a neutral beam, consisting of full, half and third energy components, with a mirror plasma is analyzed. The beam-plasma interaction is assumed to occur via ionization and charge exchange collisions. The plasma was approximated as being spherical in shape, having a uniform density, isotropic velocity distribution, and a mirror plasma energy distribution. It was found that to a first approximation, for plasma energies less than 100 keV, the charge exchange power poss (per injected atom) of the half energy component is at least twice that of the full energy component. For the third energy component, the loss is at least three times that of the full energy component. For some plasma conditions, the neutral beam can act as an energy sink for the plasma due to these charge exchange losses.

---

*This work was performed under the auspices of the United States Energy Research & Development Administration.

INTRODUCTION

The use of neutral beam injection to heat and sustain magnetically confined plasmas is a technique that is widely employed in present fusion experiments and is proposed for future fusion reactors. The injected neutral beam is attenuated in the plasma by ionization and charge exchange collisions. The fraction of the beam that is unattenuated (the penetrating beam) plus the charge exchange neutrals that do not undergo ionization emerge from the plasma and impact the wall surrounding the plasma (the first wall). Modeling of the neutral beam-plasma interaction is required to determine the mass and energy deposition rates in the plasma and on the first wall. Charge exchange has the particularly troublesome aspects that (1) it results in an additional heat load on the first wall, and (2) a given injected neutral may charge exchange with a more energetic plasma ion, resulting in a net energy loss from the plasma.

The anticipated needs of fusion research and technology will require injected neutrals with energies in the range of 10-500 keV. Present sources produce neutral beams with a particle energy distribution that is strongly peaked at several distinct values [1, 2]. The primary components of the beam occur at full energy ($\tilde{E}_0$) and at one-half ($\tilde{E}_0/2$) and one-third ($\tilde{E}_0/3$) the full energy. The energy distribution of the neutral beams may be expressed as

$$I_0 = \sum_{j=1}^{3} I_{0j}\, \delta(E_0 - \tilde{E}_0/j) \,, \qquad (1)$$

where E_o is the energy coordinate for the injected neutrals, δ is the Dirac delta function and I_{oj} is the current of the j^{th} component. Since the charge exchange cross section increases with decreasing collision energy in the 10-500 keV regime, the half and third energy neutrals have the potential for an increased amount of charge exchange with the plasma as compared to the full energy neutrals.

A previous analysis [3] has examined the interaction between a monoenergetic neutral beam and a magnetic mirror plasma, where the injected energy was equal to the most probable plasma energy (that is, the energy corresponding to the peak of the plasma energy distribution). In the present study, the analysis is extended to include the low energy components of present day neutral beam sources.

DESCRIPTION OF THE BEAM-PLASMA INTERACTION

The target for the neutral beam is assumed to be a spherical plasma of radius r_p, and the neutral beam is injected diametrically across the plasma as shown in Figure 1. Since the injected neutrals do not undergo a significant number of collisions with one another, the interaction of each beam component with the plasma was analyzed separately, and the results superposed to determine the net beam-plasma interaction. Each component of the injected beam is modeled as a monoenergetic source with energy $\tilde{E}_o/j$ and having a particle current given by I_{oj}. The beam cross section A_o is assumed to be small compared to (πr_p^2).

The primary mechanisms that attenuate the injected beam are assumed to be ionization and charge exchange collisions between the injected neutrals and the plasma ions. The injected neutrals that do not undergo

a collision emerge from the plasma and are termed penetrating neutrals. Those injected particles that experience ionization collisions are trapped in the magnetic field and contribute a net energy and mass addition to the plasma. An injected neutral that experiences a charge exchange collision creates a new neutral that has a velocity vector equal to the ion velocity vector before the collision. This "first generation" charge exchange neutral can be subsequently ionized and trapped, can escape from the plasma if it does not undergo a collision, or may experience another charge exchange collision, resulting in a "second generation" charge exchange neutral. The possibilities for the history of a second generation charge exchange neutral is the same as for the first generation, giving rise to successive generations of charge exchange neutrals. In the present study, consideration is given to only the first generation charge exchange neutrals, in that it is assumed that these particles are either ionized or escape from the plasma. The creation of subsequent generations of charge exchange neutrals is neglected; this is an acceptable approximation when the charge exchange mean free path is of order, or larger than, the plasma dimensions. Also, it should be noted that this approximation results in an upper bound on the number of charge exchange neutrals escaping from the plasma.

BEAM-PLASMA INTERACTION MODEL

The objective of the present analysis is to formulate a model that determines the fraction of the injected current that is not trapped in the plasma. This quantity is required (1) to size the neutral beam injectors (plasma physics considerations specify the required trapped current), and (2) to provide adequate heat removal capability in the reactor first wall, which must absorb the energy of the neutrals emerging

from the plasma.

In this study and its precursor [3], the details of the beam-plasma geometry, the spatial ion density distribution, and the ion angular velocity distribution are not included. The resulting model, though incomplete, preserves the most significant physical aspects of the beam-plasma interaction as described below, and provides approximate results for use in preliminary design studies.

The spherical plasma is assumed to have a uniform density n_p of a single ion specie, an ion energy distribution $f_p(E_p)$, and an isotropic velocity distribution. The determination of the energy distribution is coupled to the injection problem, in that the gross characteristics of the ion energy distribution in a mirror fusion plasma is determined by the energy of the (trapped) injected neutrals. This result is a consequence of the fact that the neutrals are the primary energy source for the plasma, and thermalization of the ions does not occur before they escape from the magnetic well. Thus, mirror plasma energy distributions are typically quite peaked at the injection energies. In this study, an approximate approach has been employed. We assume a specific functional form for $f_p(E_p)$, which was calculated on the assumption of a monoenergetic neutral source. Thus the assumed distribution function does not reflect the effects of charge exchange or the source contributions of the half and the third energy neutrals. However, the assumed distribution function should be sufficiently accurate to yield useful results for the situation where the full energy component contains most of the beam power ($\lesssim$ 100 keV for present neutral beam sources).

In the following development, we first determine the rate at which

the collisional processes in the plasma attenuate the injected beam, and then evaluate the two components of the neutral current escaping from the plasma: the penetrating neutrals and the charge exchange neutrals.

Referring to Figure 1, the injected neutral current, I, at a position x in the uniform plasma may be expressed in the form [4, 5]

$$I(x) = I_o \, e^{-x/\lambda_t} \quad . \tag{2}$$

Here, I_o is the injected current at $x = 0$ and λ_t is the total collisional mean free path for an injected neutral,

$$\frac{1}{\lambda_t} = \frac{1}{\lambda_{cx}} + \frac{1}{\lambda_i} \quad , \tag{3}$$

where the subscripts "cx" and "i" denote charge exchange and ionization, respectively.

For an arbitrary collisional process, denoted by the subscript "s", the mean free path for the neutral is

$$\lambda_s = \frac{v_o}{n_p \langle \sigma_s v_c \rangle} \quad , \tag{4}$$

where v_o is the speed of the injected neutral, $v_o = \sqrt{2E_o/m_o}$, m_o is the mass of the injected particle and $\langle \sigma_s v_c \rangle$ is the rate coefficient for the process "s". The rate coefficient is an integral of the product $\sigma_s v_c$ over the velocity distributions of the two colliding species, where σ_s is the velocity dependent cross section for the process and $v_c (= |\vec{v}_o - \vec{v}_p|)$ is the relative speed between the colliding particles.

$$\langle \sigma_s v_c \rangle = \int\int f_o(\vec{v}_o)\, f_p(\vec{v}_p)\, \sigma_s\left(\left|\vec{v}_o - \vec{v}_p\right|\right) \left|\vec{v}_o - \vec{v}_p\right| \, d\vec{v}_o d\vec{v}_p . \tag{5}$$

In the present situation involving the collision of a monodirectional monoenergetic neutral (that is, one of the injected beam components) with a plasma which is assumed isotropic in velocity space, the rate coefficient becomes [4]

$$\langle \sigma_s v_c \rangle = \int f_p(E_p) \left[\frac{1}{2} \int_0^{\pi} v_c\, \sigma_s(v_c)\, \sin\theta\, d\theta \right] dE_p , \tag{6}$$

where θ is the angle between the neutral particle and ion velocity vectors. The collision velocity is

$$v_c = \left(v_o^2 + v_p^2 - 2 v_o v_p \cos\theta \right)^{1/2} , \tag{7}$$

where v_p is the ion speed, $v_p = \sqrt{2E_p/m_p}$, and m_p is the ion mass.

Introducing the nondimensional space coordinate

$$\xi = \frac{x}{2r_p} , \tag{8}$$

the injected neutral particle current in the plasma, Eq. (2), becomes

$$I(\xi) = I_o\, e^{-\gamma\xi} , \tag{9}$$

where the plasma attenuation parameter, γ, is defined as

$$\gamma = \frac{2r_p}{\lambda_T} . \tag{10}$$

This quantity can be rewritten explicitly in terms of the rate coefficients as

$$\gamma = (n_p \ell)\left[\frac{\left(\langle \sigma_i v_c \rangle + \langle \sigma_{cx} v_c \rangle\right)}{v_o}\right] , \tag{11}$$

where $\ell = 2r_p$. The attenuation coefficient can, therefore, be separated into the product of the plasma line density, $n_p \ell$, and a function dependent on the energetics of the collisional interaction. The quantity in brackets in Eq. (11) is an energy averaged cross section,

$$\sigma_T(E_o, \tilde{E}_p) = \frac{\left(\langle \sigma_i v_c \rangle + \langle \sigma_{cx} v_c \rangle\right)}{v_o} , \tag{12}$$

and is a function of the injection energy, E_o, and the characteristic plasma energy, $\tilde{E}_p$ (which will be explicitly defined later in the development).

The fraction of the neutral beam which penetrates the plasma may now be evaluated directly from Eq. (9) by setting $\xi = 1$. For the j^{th} component of the beam, this fraction is

$$\frac{I_{pj}}{I_{oj}} = \bar{e}^{\,\gamma_j} , \tag{13}$$

where I_{pj} is the j^{th} current component that penetrates the plasma and γ_j is the plasma attenuation coefficient for $E_o = \tilde{E}_o/j$.

The geometric variables for formulating the charge exchange loss from the plasma are shown in Figure 1. We consider the collision of neutral particles of velocity v_o with the plasma ions at a position x on the beam axis. The rate of production of charge exchange neutrals which have velocity vectors in the interval $(\vec{v}_p, d\vec{v}_p)$ is

$$d^3\dot{n}_{cx}(x,\vec{v}_p) = n_o(x)\left[n_p f_p(\vec{v}_p)d\vec{v}_p\right] v_c\sigma_{cx}(v_c), \tag{14}$$

where $n_o(x) = I(x)/v_o A_o$ is the injected particle density at point x, and the quantity in brackets is the ion density in the $(\vec{v}_p,d\vec{v}_p)$ interval of velocity space. Transforming the isotropic ion velocity distribution to the coordinates (E_p,θ,ϕ) yields,

$$f_p(\vec{v}_p)d\vec{v}_p = f_p(E_p)dE_p \cdot \frac{1}{4\pi} \sin\theta\, d\theta\, d\phi, \tag{15}$$

where ϕ is the azimuthal angle. Invoking the azimuthal symmetry of the problem, Eq. (14) is integrated over ϕ resulting in an expression for the rate of production of charge exchange neutrals at the position x with energy in the interval (E_p,dE_p) having direction in the interval $(\theta,d\theta)$

$$d^2\dot{n}_{cx}(x,E_p,\theta) = n_o(x)\left[n_p f_p(E_p)dE_p \cdot \frac{1}{2}\sin\theta d\theta\right] v_c\sigma_{cx}(v_c). \tag{16}$$

The rate of escape of these first generation charge exchange neutrals from the plasma is

$$d^2\dot{n}_{cx}(r_p,x,E_p,\theta) = d^2\dot{n}_{cx}(x,E_p,\theta)\, e^{-y/\lambda_i^*}, \tag{17}$$

where y is shown in Figure 1, and is the path length from the point of origination of the charge exchange neutral to the plasma surface. In Eq. (17), λ_i^* is the ionization mean free path for the charge exchange neutral,

$$\frac{1}{\lambda_i^*} = \frac{n_p}{v_p}\int f_p(E_p')\left[\frac{1}{2}\int_o^{\pi} v_c'\,\sigma_i(v_c')\,\sin\theta' d\theta'\right] dE_p', \tag{18}$$

where

$$v_c' = \left(v_p^2 + (v_p')^2 - 2v_p v_p' \cos\theta'\right)^{1/2}. \tag{19}$$

The prime indicates an integration over the plasma velocity coordinates with respect to a neutral having velocity v_p and direction θ. The differential flux of neutrals in the class (E_p, dE_p) and (θ,$d\theta$) through the surface dA_p, due to charge exchange reactions in the differential volume dV centered at x, is then

$$d^3 I_{cx}(x,E_p,\theta) = d^2\dot{n}_{cx}(r_p,x,E_p,\theta)\, dV, \tag{20}$$

where $dV = A_o\, dx$. Using the previously developed relations, the differential charge exchange particle flux through the plasma surface may be expressed as

$$d^3 I_{cx}(\xi,E_p,\theta) = \frac{I_o \gamma}{2} \frac{\sigma_{cx}(v_c)v_c}{\langle \sigma v_c \rangle_T} e^{-(\gamma\xi + y/\lambda_i^*)} f_p(E_p)\sin\theta\, dE_p\, d\theta\, d\xi, \tag{21}$$

where

$$\langle \sigma v_c \rangle_T = \langle \sigma_i v_c \rangle + \langle \sigma_{cx} v_c \rangle. \tag{22}$$

The energy flux carried by the escaping charge exchange neutrals is the product of the particle flux and the particle energy E_p,

$$d^3 P_{cx}(\xi,E_p,\theta) = E_p d^3 I_{cx}(\xi,E_p,\theta). \tag{23}$$

The total particle and energy loss from the plasma due to charge exchange is now found by integrating Eqs. (21) and (23) over space, energy and angle,

$$I_{cx} = \int_{\xi=0}^{1} \int_{\theta=0}^{\pi} \int_{E_p=0}^{\infty} d^3 I_{cx}(\xi, E_p, \theta), \tag{24}$$

$$P_{cx} = \int_{\xi=0}^{1} \int_{\theta=0}^{\pi} \int_{E_p=0}^{\infty} E_p d^3 I_{cx}(\xi, E_p, \theta). \tag{25}$$

Equations (14) - (25) have been formulated for an injected beam of arbitrary energy E_o and current I_o. To obtain results for the specific beam described by Eq. (1), the equations must be evaluated for the energies $E_o = E_o/j$ $(j = 1,2,3)$ and currents $I_o = I_{oj}$. The total charge exchange current power losses are then the sum of the three components,

$$\frac{I_{cx}}{I_o} = \sum_{j=1}^{3} \chi_j \left(\frac{I_{cxj}}{I_{oj}} \right) \tag{26}$$

$$\frac{P_{cx}}{P_o} = \sum_{j=1}^{3} \psi_j \left(\frac{P_{cxj}}{P_{oj}} \right), \tag{27}$$

where the current and power fractions in the beam, χ_j and ψ_j, respectively, are defined as

$$\chi_j = I_{oj}/I_o, \tag{28}$$

$$\psi_j = P_{oj}/P_o = \frac{\left(\chi_j/j\right)}{\sum_{j=1}^{3} \left(\chi_j/j\right)}, \tag{29}$$

and

$$P_{oj} = \left(\tilde{E}_o/j\right) I_{oj}, \tag{30}$$

$$P_o = \sum_{j=1}^{3} P_{oj}, \tag{31}$$

$$I_o = \sum_{j=1}^{3} I_{oj}. \tag{32}$$

The total neutral beam current and power escaping the plasma is due to charge exchange and penetration and is found by summing the two contributions.

$$\frac{I_T}{I_o} = \frac{I_{cx}}{I_o} + \frac{I_p}{I_o}, \tag{33}$$

$$\frac{P_T}{P_o} = \frac{P_{cx}}{P_o} + \frac{P_p}{P_{cx}}, \tag{34}$$

where the penetrating contributions are

$$\frac{I_p}{I_o} = \sum_{j=1}^{3} \chi_j \left(\frac{I_{pj}}{I_{oj}}\right), \tag{35}$$

$$\frac{P_p}{P_o} = \sum_{j=1}^{3} \psi_j \left(\frac{P_{pj}}{P_{oj}}\right) \tag{36}$$

Note that $\left(P_{pj}/P_{oj}\right) = \left(I_{pj}/I_{oj}\right)$, since these particles emerge from the plasma with the energy at which they were injected.

CALCULATIONAL RESULTS

To apply the model developed above, it is necessary to specify the plasma energy distribution, the velocity dependent cross sections, and the plasma parameters n_p and ℓ.

The plasma energy distribution is selected to be typical of a mirror plasma sustained by a monoenergetic source. The following expressions for a mirror ratio of R = 3, given by Riviere [4], are used.

$$f(\varepsilon_p) = 0 \qquad \varepsilon_p < 0.18;\ \varepsilon_p > 2.5$$

$$f(\varepsilon_p) = -1.316\ \varepsilon_p^2 + 2.831\ \varepsilon_p - 0.4574 \qquad 0.18 < \varepsilon_p < 1 \tag{37}$$

$$f(\varepsilon_p) = 1.684 - 1.0526 \left[-3.69 + 5\varepsilon_p - \varepsilon_p^2\right]^{1/2} \qquad 1 < \varepsilon_p < 2.5$$

Here, ε_p is a normalized plasma energy,

$$\varepsilon_p = \frac{E_p}{\tilde{E}_p}, \tag{38}$$

and $\tilde{E}_p$ is the most probable plasma energy (i.e., the energy corresponding to the peak of the plasma energy distribution), which we equate to the energy of the full energy component of the injected beam,

$$\tilde{E}_p = \tilde{E}_o. \tag{39}$$

The data for the ionization and charge exchange cross sections for hydrogen have been curve-fit by Riviere [4]. The equations for the ionization cross section (in units of cm^2) are

$$\log_{10} \sigma_i = -0.8712 \left(\log_{10} E_c^H\right)^2 + 8.156 \left(\log_{10} E_c^H\right) - 34.833, \tag{40}$$

$$10^3 < E_c^H < 1.5 \times 10^5,$$

$$\sigma_i = \frac{3.6 \times 10^{12}}{E_c^H} \log_{10}\left(0.1666 E_c^H\right) \quad 1.5 \times 10^5 < E_c^H < 10^6. \tag{41}$$

The quantity E_c^H is the collision energy, in eV., of the proton-hydrogen atom collision pair,

$$E_c^H = \frac{1}{2e} m_H v_c^2, \tag{42}$$

where e is the electron charge and m_H the proton mass. Since the cross section for this process is only a function of v_c, i.e., $\sigma_i(v_c)$, Eqs. (40) and (41) can be used to evaluate the cross section for an ionizing collision between any of the hydrogen isotopes, as long as it is noted that E_c^H is not the actual collision energy but rather is the quantity defined in Eq. (42). The curve-fit was used below 10^3 eV, although Riviere did not show data in this energy region. For charge exchange, the cross section (in units of cm^2) is

$$\sigma_{cx} = \frac{0.6937 \times 10^{-14}\left[1 - 0.155 \log_{10} E_c^H\right]^2}{1 + 0.1112 \times 10^{-14}\left(E_c^H\right)^{3.3}}, \quad E_c^H > 10^2, \tag{43}$$

where, again, E_c^H is defined via Eq. (42). For $E_c^H < 10^2$, σ_{cx} was evaluated at $E_c^H = 10^2$. The values of the two cross sections calculated from these curve fits are shown in Figure 2. It can be seen that below 10 keV (equivalent hydrogen collision energy, E_c^H), the neutral-ion interaction is dominated by the charge exchange mechanism. Between 10 and 100 keV, ionization and charge exchange are the same order of magnitude, with ionization becoming increasingly more important with increasing energy. Above 100 keV, ionization is dominant.

Using these cross sections, the plasma attenuation parameter can be evaluated, and this quantity is shown in Figure 3 for the three beam components as a function of most probable plasma energy for a plasma line density of 10^{15} cm^{-2}. These parameters are decreasing functions of plasma energy, as would be anticipated from the energy dependence of the total cross section shown in Figure 2. The curves appearing in Figure 3 are convenient for estimating the beam-plasma coupling via Eq. (13). Since γ_j is linear in $n_p\ell$ (see Eq. [11]), the curves in Figure 3 may be used to obtain γ_j for any plasma simply by multiplying the value obtained from the figure by the line density in units of 10^{15} cm^{-2}.

Of those neutrals that collide with the plasma, determined by the parameter γ_j, some are ionized and trapped and the remainder are charge exchanged. To examine the comparative magnitudes of these two processes, it is useful to examine the quantity

$$\left(\frac{\lambda_s}{\ell}\right)_j = \frac{(v_o)_j}{n_p \ell \left(\langle \sigma_s v_c \rangle\right)_j} \quad , \tag{44}$$

which is the mean free path for a neutral of energy $\tilde{E}_o/j$ undergoing process "s", normalized on the characteristic plasma dimension. It is convenient to generalize this quantity by multiplying it by the plasma attenuation coefficient, γ_j, which removes the plasma line density from the result,

$$(\Lambda_s)_j = \frac{(\lambda_s)_j}{\ell} \gamma_j . \tag{45}$$

This density independent mean free path is just a function of collisional energetics,

$$(\Lambda_s)_j = \frac{(\langle \sigma v_c \rangle_T)}{(\langle \sigma_s v_c \rangle)_j^j}, \tag{46}$$

and is shown in Figure 4 for the ionization and charge exchange reactions. The value of $(\lambda_s/\ell)_j$ is thus simply obtained by dividing the value of $(\Lambda_s)_j$ from the figure by γ_j. Using plasma data from conceptual mirror reactor studies [6, 7, 8] yields values for the plasma attenuation coefficient in the range $1 \lesssim \gamma_j \lesssim 10$.

The significance of the nondimensional mean free path is that $(\lambda_s/\ell) << 1$ indicates a strong beam-plasma interaction via collisional mechanism "s" and $(\lambda_s/\ell) >> 1$ implies a weak interaction. Bearing in mind the range of γ_j cited above, it can be seen from Figure 4 that at low plasma energies ($\tilde{E}_p \lesssim 50$ keV), most of the beam attenuation occurs due to charge exchange, and the charge exchange neutrals will have a large probability of escape from the plasma due to the large ionization mean free path. With increasing energy, ionization becomes a stronger effect and charge exchange less important. Above approximately 100 keV, the beam attenuation is caused primarily by ionization.

We may therefore summarize our semi-quantitative picture of the beam-plasma interaction in the following fashion. The neutral beam attenuation is a decreasing function of most probable plasma energy, $\tilde{E}_p$, in the range $10 \lesssim \tilde{E}_p \lesssim 500$ keV. However, at the lower energies, the comparatively large beam attenuation is caused by charge exchange, with the resulting neutrals escaping from the plasma and thus yielding no net addition to the plasma. With increasing energy, ionization accounts for

an increasing fraction of the beam attenuation, and above approximately 100 keV, charge exchange becomes a second order effect as compared to ionization. Note that the quantities that quantify these concepts, (γ_j), $(\lambda_i/\ell)_j$ and $(\lambda_{cx}/\ell)j$ can be readily evaluated for any plasma from Figures 3 and 4 by specifying the plasma line density, $n_p\ell$, and the plasma energy, $\tilde{E}_p$.

Having established a physical picture of the interaction, we are now in a position to interpret the results of the complete formulation, as given by Eq's. (24) and (25). The charge exchange current loss from the plasma, normalized to the injected current, is plotted as a function of $\tilde{E}_p$ for the three beam components in Figure 5. In this figure, γ_1 was held constant. At a given value of $\tilde{E}_p$, the curves for the three components correspond to interaction with the same plasma, i.e., the same value of $n_p\ell$ as determined from Eq. (11). The charge exchange loss is a strongly decreasing function of $\tilde{E}_p$ as was anticipated from the charge exchange mean free path argument presented previously. The larger charge exchange loss for the $j = 2$ and 3 components as compared to the $j = 1$ component is also explained from Figure 4, where it is seen that the half and third energy neutrals have smaller charge exchange mean free paths than the full energy neutrals.

The total current loss from the plasma (charge exchange plus penetration) is shown in Figure 6. For the primary beam component, this curve is about .05 higher than the corresponding charge exchange curve in Figure 5, since $e^{-3} = 0.05$. There is a slightly smaller difference between the charge exchange and total current loss curves for the other two beam components because of the larger values of γ_j (shown in Figure 3) for these components.

The power loss from the plasma for the three components, normalized to the injected power of the component, is shown in Figure 7. These results illustrate a very detrimental condition caused by the two beam components not at the primary energy: these neutrals, for low $\tilde{E}_p$ are an energy sink rather than source for the plasma. This situation occurs because most of the ions in the plasma have energy greater than the energy of the injected neutrals in the half and third energy beam components. Thus charge exchange collisions between these neutrals and plasma ions result, on the average, in the release from the plasma of a more energetic neutral than was injected.

The net charge exchange interaction of the beam with the plasma, which is the weighted sums of the three components given in Eq's. (26) and (27), are now evaluated. The current and power fractions, χ_j and ψ_j, are taken from [1,9] and are typical of the LBL positive ion neutral beam source [10]. The current fractions are shown in Figure 8 up to an energy of $\tilde{E}_0$ = 200 keV; above this energy, positive ion sources become too inefficient for use in a reactor system [6]. The power fractions are related to χ_j via Eq. (29).

The charge exchange current loss for the total beam, Eq. (26), is shown in Figure 9 for the range of plasma energies and plasma attenuation coefficients of interest. At low energy, the charge exchange loss displays a maximum at $\gamma_1 = 3$, and at high energy, the loss is a decreasing function of γ_1.

The charge exchange loss from the plasma is significant only when (1) the normalized charge exchange mean free path (λ_{cx}/ℓ) is small,

causing significant charge exchange attenuation of the injected beam, and (2) the normalized ionization mean free path (λ_i/ℓ) is large, precluding ionization and trapping of the charge exchange neutrals. The values of these two quantities can be evaluated from Figure 4, where the mean free path λ/ℓ is obtained by dividing Λ by γ. For the low energy range of Figure 9, significant charge exchange attenuation of the injected beam occurs over the range of γ_1 shown since $(\lambda_{cx}/\ell) < 1$. The $\gamma_1 = 3$ curve exhibits a higher fractional loss than the $\gamma_1 = 1$ curve since at this larger γ_1 there is more charge exchange attenuation, and the ionization mean free path is large enough to allow most of the charge exchange neutrals to escape from the plasma. The $\gamma_1 = 10$ curve lies below the $\gamma_1 = 3$ curve because in this case the ionization mean free path is small enough to cause ionization of a significant fraction of the charge exchange neutrals and thus prevent their escape from the plasma. At the higher energies, the ionization mean free path is small enough that the charge exchange loss decreases as γ_1 increases.

The charge exchange power loss for the total beam, corresponding to the curves of current in Figure 9, are shown in Figure 10. The power loss at low energies associated with the half and third energy beam components (shown in Figure 7) result in a net power removal by the beam from the plasma for $\tilde{E}_p \lesssim 15$ keV and $\gamma_1 = 3$ and 10.

CONCLUSION

It was anticipated that charge exchange losses due to the half and third energy components of present day neutral beams would be larger than the full energy beam component based on the following considerations:

(1) The charge exchange cross section is a decreasing function

of energy. Thus a lower energy neutral, i. e., half and third energy, will have a larger probability of a charge exchange reaction than a full energy neutral.

(2) Since most plasma ions have greater energy than the half and third energy neutrals, charge exchange reactions between these particles can result in a net energy loss from the plasma.

These effects have been quantified in the present analysis, and a range of plasma conditions typical of mirror reactors were examined with the model. It was found that for plasma energies $\lesssim$ 50 keV, there are some conditions where the half and third energy neutrals cause a net energy removal from the plasma. To a first approximation, for plasma energies less than 100 keV, the fractional charge exchange power loss $(P_{cx}/P_o)_j$ of the half energy component is at least twice that of the full energy component, and for the third energy component, the loss is at least three times that of the full energy component. Consideration of the design of mono-energetic neutral beam sources is strongly indicated by this analysis.

REFERENCES

[1] Berkner, K. H., R. V. Pyle and J. W. Stearns, "Mixed Species in Intense Neutral Beams", Lawrence Berkeley Laboratory, Report No. LBL-2469, 1974; also Proceedings of the First Topical Meeting on the Technology of Controlled Nuclear Fusion, AEC CONF.-740402-P1, 1974.

[2] Stewart, L. D., et al, "Neutral Beam Injection Heating of ORMAK", Paper E12, 3rd Int. Symp. Toroidal Plasma Confinement, Max-Planck-Institut für Plasma-Physik, Garching, 1973.

[3] Carlson, G. A. and G. W. Hamilton, "Wall Bombardment Due to the Charge Exchange of Injected Neutrals with a Fusion Plasma", Lawrence Livermore Laboratory, Report No. UCRL-75306, 1974; also Proceedings of the First Topical Meeting on the Technology of Controlled Nuclear Fusion, AEC CONF.-740402-P1, 1974.

[4] Riviere, A. C., "Penetration of Fast Hydrogen Atoms into a Fusion Reactor Plasma," Nuclear Fusion, Vol. 11, p. 363, 1971.

[5] Hovingh, J. and R. W. Moir, "Efficiency of Injection of High Energy Neutral Beams into Thermonuclear Reactors," Lawrence Livermore Laboratory, Rpt. No. UCRL-51419, July, 1973.

[6] Werner, R. W., G. A. Carlson, J. Hovingh, J. D. Lee and M. A. Peterson, "Progress Report #2 on The Design Considerations for a Lower Power Experimental Mirror Fusion Reactor," Lawrence Livermore Laboratory, Rpt. No. UCRL-74054, 1973.

[7] Batzer, T. H., et al, "Conceptual Design of a Mirror Reactor for a Fusion Engineering Research Facility (FERF)," Lawrence Livermore Laboratory, Rpt. No. UCRL-51617, 1974.

[8] R. W. Moir, et al, "Progress on the Conceptual Design of a Mirror *Hybrid Fusion-Fission Reactor*," Lawrence Livermore Laboratory, Report in preparation, 1975.

[9] Berkner, K. H., et al, "Neutral Beam Development and Technology: Program Plan and Major Project Proposal, "Lawrence Livermore Laboratory, Rpt. No. LLL Prop.-115, September 1974.

[10] Baker, W. R., et al, "Neutral Beam Research and Development at LBL, Berkeley," Proc. of 5th Symposium on Engineering Problems of Fusion Research, IEEE Pub. No. 73CH0843-3 NPS, pg. 413 (1973).

FIGURE CAPTIONS

Fig. 1 Beam-plasma geometry.

Fig. 2 Ionization and charge exchange cross sections.

Fig. 3 Plasma attenuation parameter for D injected into D^+.

Fig. 4 Density independent mean free path.

Fig. 5 Fractional current loss of injected beam due to charge exchange for D injected into D^+.

Fig. 6 Fractional current loss of injected beam due to charge exchange and penetration for D injected into D^+.

Fig. 7 Fractional power loss of injected beam due to charge exchange for D injected into D^+.

Fig. 8 Current fractions in the positive ion neutral beam.

Fig. 9 Fractional current loss for the sum of the 3 beam components due to charge exchange for D injected into D^+.

Fig. 10 Fractional power loss for the sum of the 3 beam components due to charge exchange for D injected into D^+.

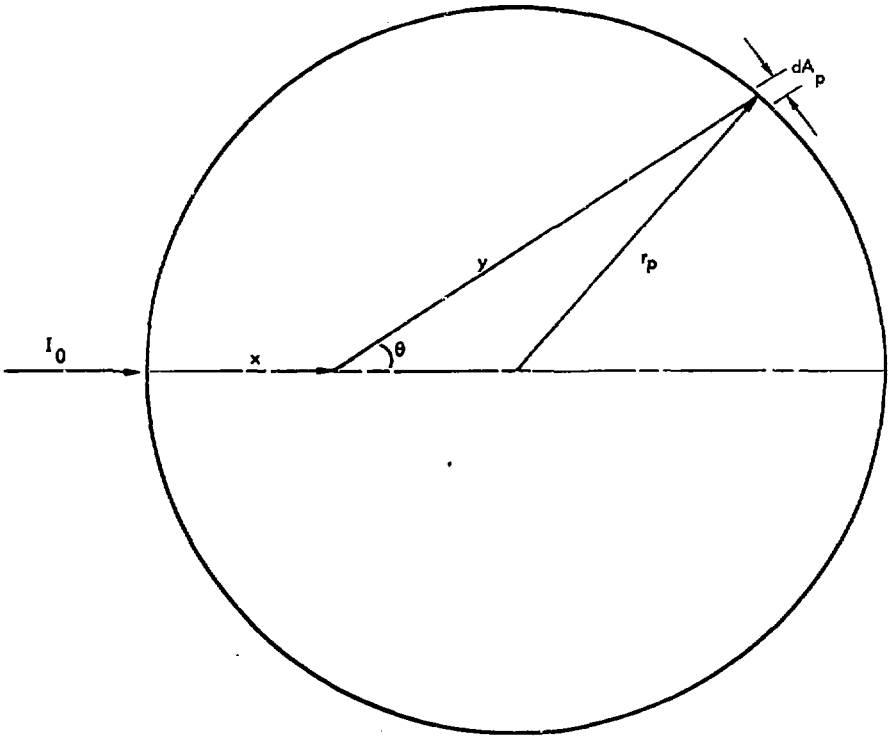

Fig. 1

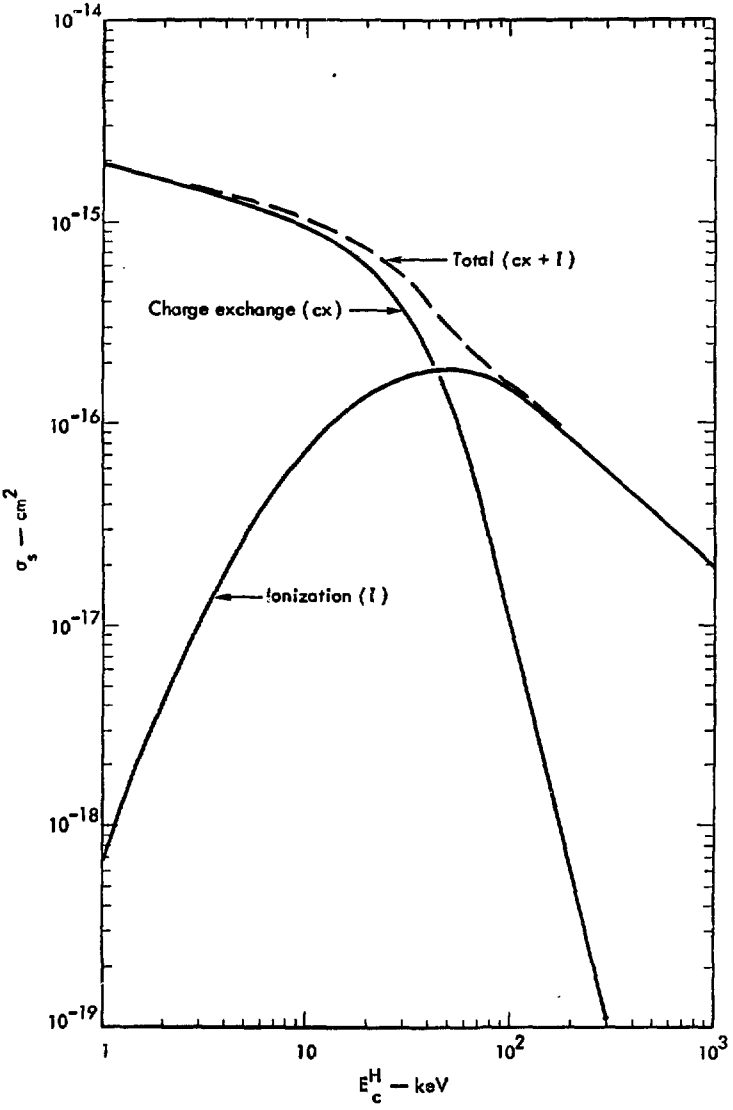
10^{-14}
10^{-15}
10^{-16}
10^{-17}
10^{-18}
10^{-19}
σ_s — cm^2
Total (cx + I)
Charge exchange (cx)
Ionization (I)
1
10
10^2
10^3
E_c^H — keV

Fig. 2

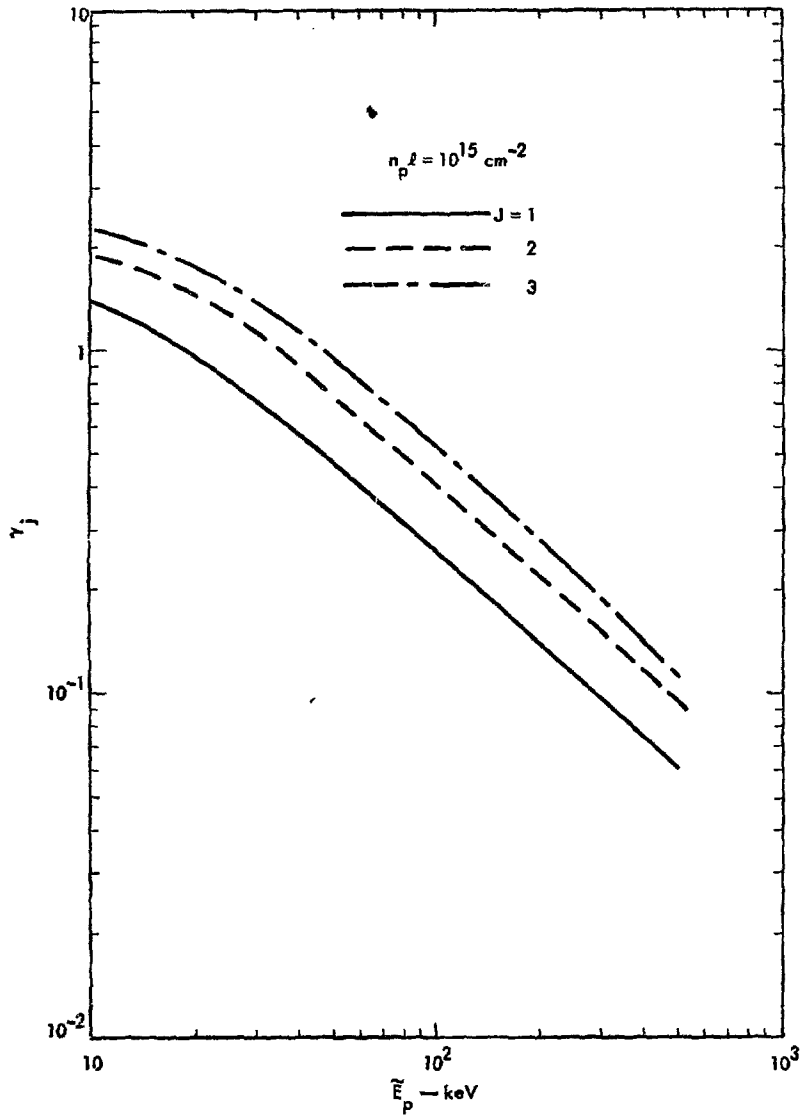

Fig. 3

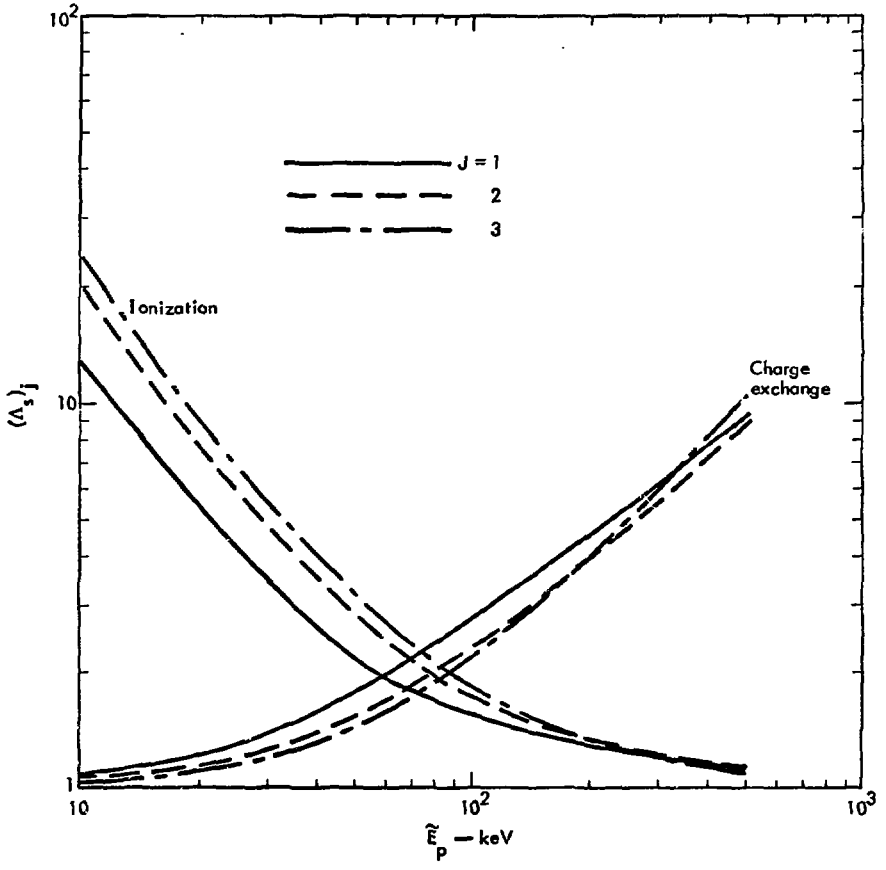
10^2
J = 1
2
3
Ionization
Charge exchange
$(\Lambda_s)_j$
10
1
10
10^2
10^3
$\tilde{E}_p$ — keV

Fig. 4

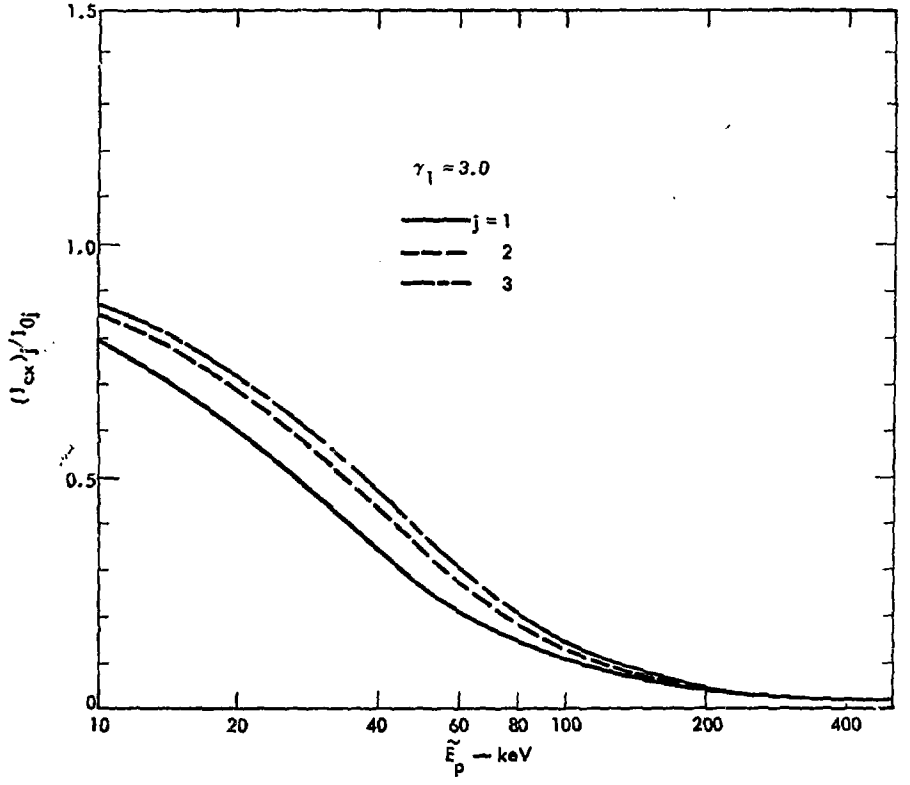
1.5
1.0
0.5
0
$\gamma_1 = 3.0$
j = 1
2
3
$(J_{cx})_j/J_{0j}$
10
20
40
60
80
100
200
400
$\tilde{E}_p$ — keV

Fig. 5

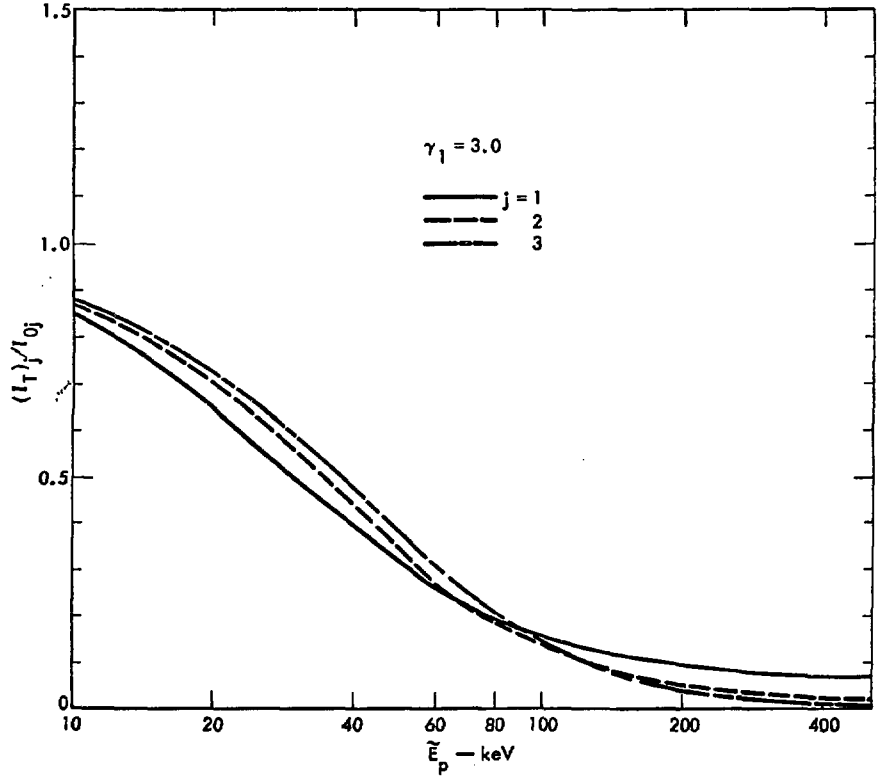
1.5
1.0
0.5
0
$\gamma_1 = 3.0$
j = 1
2
3
$(I_T)_j/I_{0j}$
10
20
40
60
80
100
200
400
$\tilde{E}_p$ — keV

Fig. 6

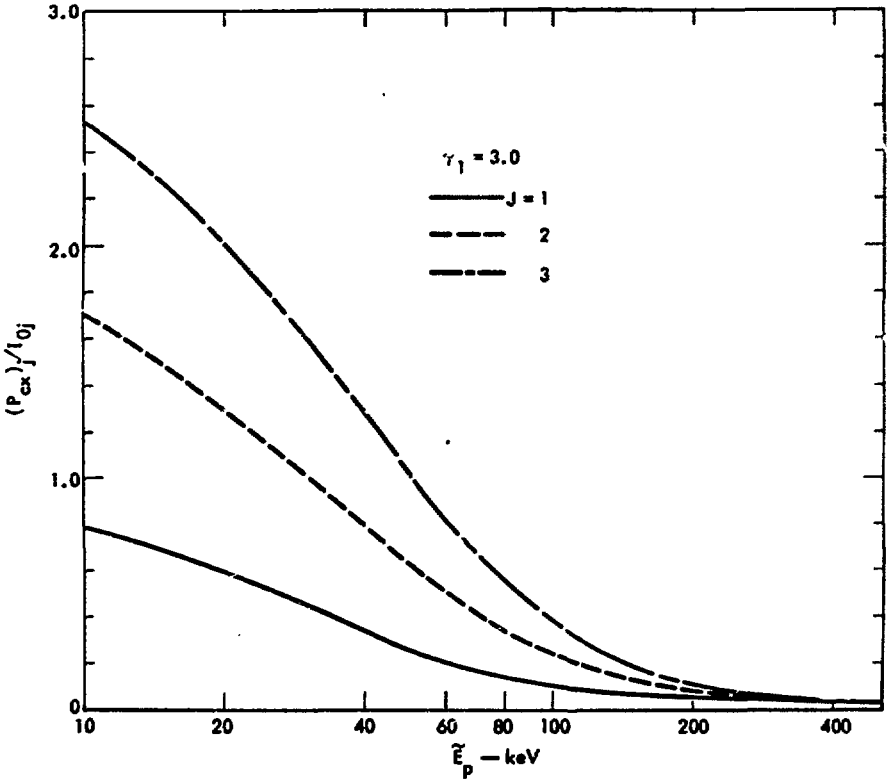
3.0
2.0
1.0
0
$(P_{ex})_j/I_{0j}$
$\gamma_1 = 3.0$
J = 1
2
3
10
20
40
60
80
100
200
400
$\tilde{E}_p$ — keV

Fig. 7

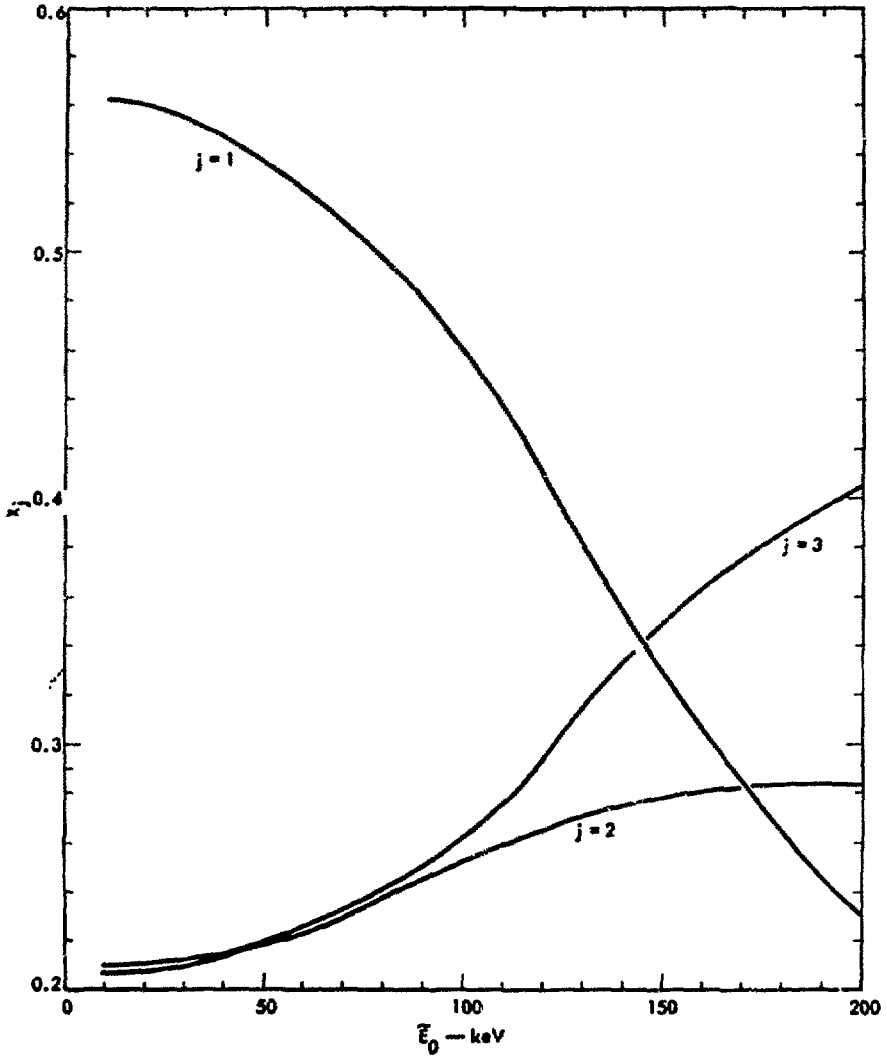

Fig. 8

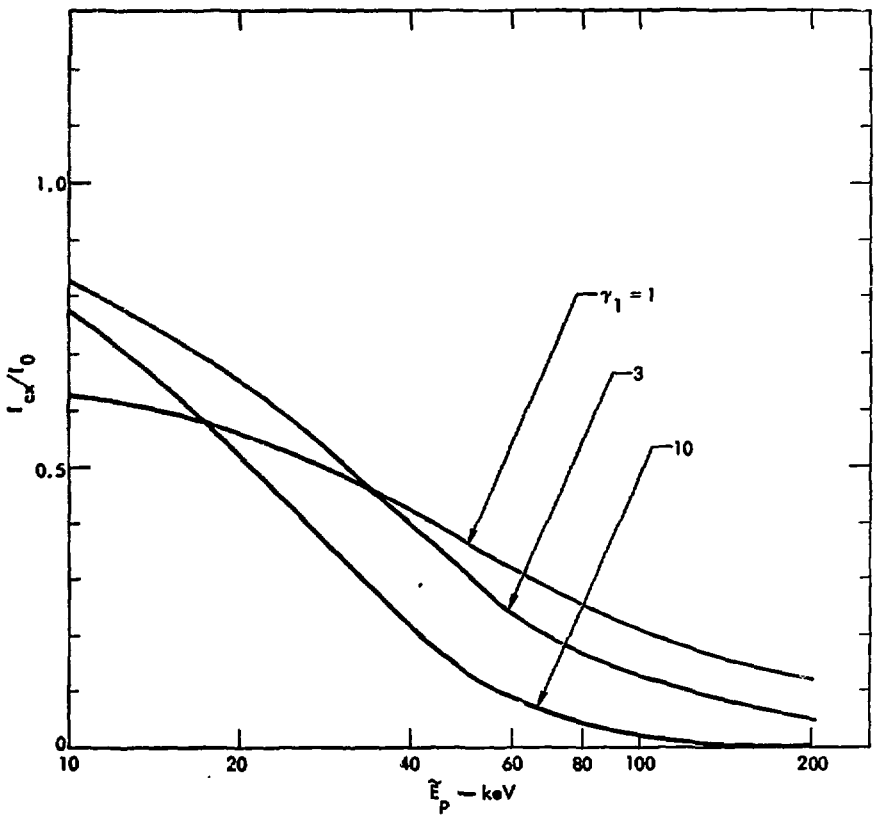

Fig. 9

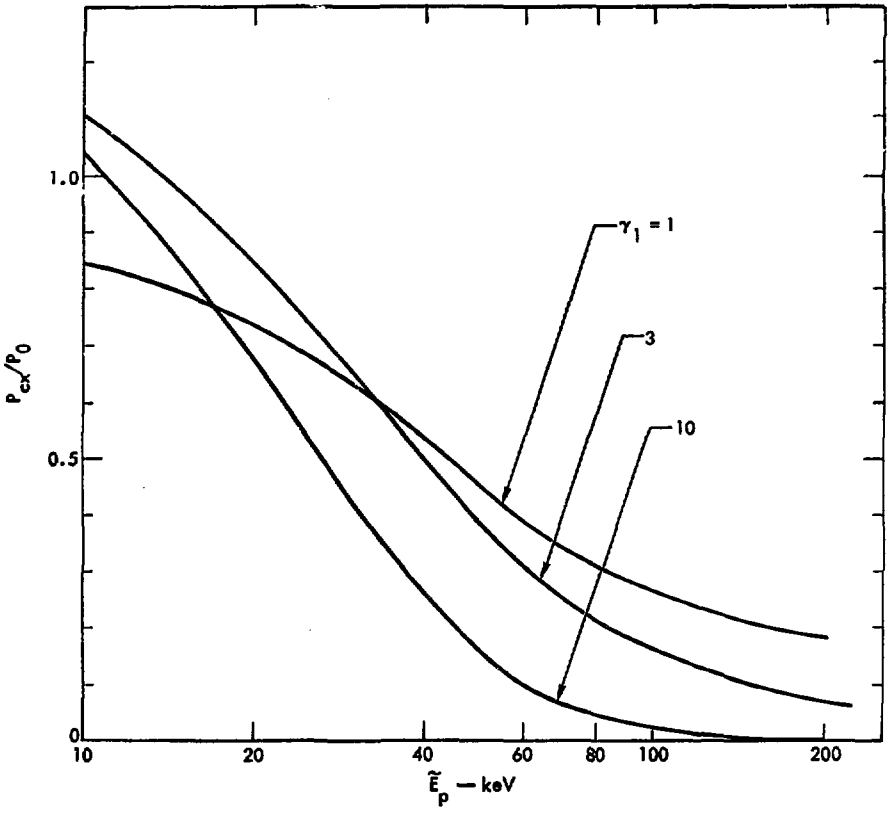

Fig. 10